pISSN 1229-3008 eISSN 2287-6251
Progress in Superconductivity and Cryogenics
Vol.17, No.4, (2015), pp.16~20 http://dx.doi.org/10.9714/psac.2015.17.4.016

Extended Drude model analysis of *n*-doped cuprate, $Pr_{0.85}LaCe_{0.15}CuO_4$

Seokbae Lee[a], Dongjoon Song[b], Eilho Jung[a], Seulki Roh[a], Changyoung Kim[b], and Jungseek Hwang[*,a]

[a] *Department of Physics, Sungkyunkwan University,Gyeonggi-do, Suwon 440-746, Korea*
[b] *Department of Physics, Yonsei University, Seoul 120-749, Korea*

(Received 16 November 2015; revised or reviewed 18 December 2015; accepted 19 December 2015)

Abstract

We investigated optical properties of an electron-doped copper oxide high temperature superconductor, $Pr_{0.85}LaCe_{0.15}CuO_4$ (PLCCO) single crystal. We obtained the optical conductivity from measured reflectance at various temperatures. We found our data contained *c*-axis longitudinal optical (LO) phonon modes due to miscut and intrinsic lattice distortion. We applied an extended Drude model to study the correlations between charge carriers in the system. The LO phonons appear as strong sharp peaks in the optical scattering rate. We tried to remove the LO phonon modes by using the energy loss function, which also shows the LO phonons as peaks, and could not remove them completely. We extracted the electron-boson spectral density function using a generalized Allen's formula. We observed that the resulting electron-boson density show similar temperature dependence as hole-doped cuprates.

Keywords: electron-doped cuprates, electron-boson spectral density, extended Drude model

1. INTRODUCTION

After the discovery [1] of the high-temperature copper oxide superconductors (cuprates) they have been studied intensively [2-5]. Electron-doped cuprates have been also discovered [6] but have been studied less than its counterpart materials, hole-doped cuprates, because of mostly its lower superconducting transition temperature and less variety of compounds. The electron-doped cuprates show a wider anti-ferromagnetic ordering phase than the hole-doped ones. The phase diagram of the cuprates shows more or less electron-hole symmetry; both undoped parent compounds show anti-ferromagnetic Mott insulating phase [7]. As doping increases in both (hole and electron doping) directions the anti-ferromagnetic phase is weakened and a superconducting phase appears. Many researchers including us believe that both electron- and hole-doped cuprates have the same superconducting mechanism. The superconducting mechanism seems to closely relate to the anti-ferromagnetic spin fluctuations because the superconducting phase locates nearby or/and coexists with the anti-ferromagnetic phase in the phase diagram [7].

In this paper we study an electron-doped $Pr_{0.85}LaCe_{0.15}CuO_4$ (PLCCO) single crystal sample using an optical spectroscopy technique. We obtained the optical conductivity of PLCCO from measured reflectance using a Kramers-Kronig relation. We observed unusual enhancement below 600cm^{-1} along with strong sharp dips in the measured reflectance. We attribute the sharp dips to longitudinal optical (LO) phonons which can appear due to the miscuts or intrinsic lattice distortions. We also applied an analysis method of reflectance spectra of strongly correlated electron systems [8]. We used an extended Drude model to obtain the optical self-energy which may carry correlation information among charge carriers and is closely related to the quasiparticle self-energy. We observed strong peaks in the optical scattering rate (or the imaginary part of the optical self-energy) which may come from LO phonon or *c*-axis transverse optical (TO) phonon contributions. We tried to extract the electron-boson spectral density functions from the optical scattering rate using a generalized Allen's formula or Shulga *et al.*'s formula [9, 10] and a maximum entropy inversion method [11, 12]. The temperature dependence of the extracted electron-boson spectral density function is similar to those of hole-doped cuprates; as lowering temperature the coupling constant increases and a broad peak position in the electron-boson spectral density decreases.

2. EXPERIMENTS

Our $Pr_{0.85}LaCe_{0.15}CuO_4$ (PLCCO) single crystal sample was grown by using a traveling solvent floating zone method using an optical furnace. The sample was annealed in high purity N_2 gas atmosphere for ~16 hours at 900 – 930 ℃. Additional air annealing was done [13]. Its superconducting transition temperature (T_c) is 21 K. The *ab*-plane sample surface was cut and polished. For this study we used a commercial FTIR spectrometer (Bruker Vertex 80v) and a continuous liquid helium flow cryostat (RG Hansen). We measured *ab*-plane reflectance of the sample at various temperatures below room temperature using an in-situ metallization technique [14]. The

* Corresponding author: jungseek@skku.edu

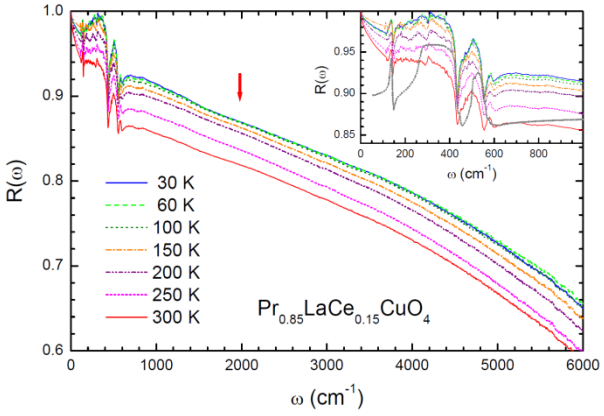

Fig. 1. Measured reflectance spectra of our PLCCO sample at various temperatures. In the inset we compare the measured reflectance spectra of $Pr_{0.85}LaCe_{0.15}CuO_4$ with a *c*-axis reflectance of $Nd_{1.85}Ce_{0.15}CuO_{4+\delta}$ in gray dashed line which is reproduced from a reported paper [17].

measured reflectance spectra are shown in Fig. 1. We note that all measured temperatures are above the T_c. The reflectance spectra show strong temperature dependence above 100 K and but below the temperature the temperature dependence is quite small. There is a very slight suppression near 2000 cm^{-1} marked with a red arrow which may be related to the pseudogap originated from antiferromagnetic spin correlation in the system [15, 16]. We observe sharp dips below 600 cm^{-1} which seem to be caused by longitudinal optical (LO) or *c*-axis phonons. In the inset we display the measured reflectance spectra below 1000 cm^{-1} and a rescaled *c*-axis reflectance spectrum $(0.1R_c(\omega) + 0.86)$ of $Nd_{1.85}Ce_{0.15}CuO_{4+\delta}$ reproduced from a reported literature [17]. We can see that the sharp dips in our *ab*-plane reflectance spectra coincide with the well-known *c*-axis phonons. But it is not clear what is the origin of the LO phonons in our *ab*-plane reflectance. The LO phonons can come from both a surface miscut [18] and lattice distortions introduced by Ce dopants of which size is different from those of Pr and La atoms.

3. RESULT AND DISCUSSIONS

We applied a Kramers-Kronig (KK) analysis to the measured reflectance and obtained the optical constants including the optical conductivity and the dynamic dielectric function. To perform the KK analysis we had to extrapolate the measured spectrum to zero and infinite frequencies. For the high frequency extrapolation we extended our data up to 22,000 cm^{-1} using reported data [16] and further extrapolations were performed appropriately [19]. For the low frequency extrapolation we used a Hagen-Rubens relation, i.e. $1 - \mathrm{R}(\omega) = A\sqrt{\omega}$, where A is a constant. The real parts of the optical conductivity spectra $(\sigma_1(\omega))$ at various temperatures are shown in the upper frame of Fig. 2. They show monotonic temperature dependence; with lowering

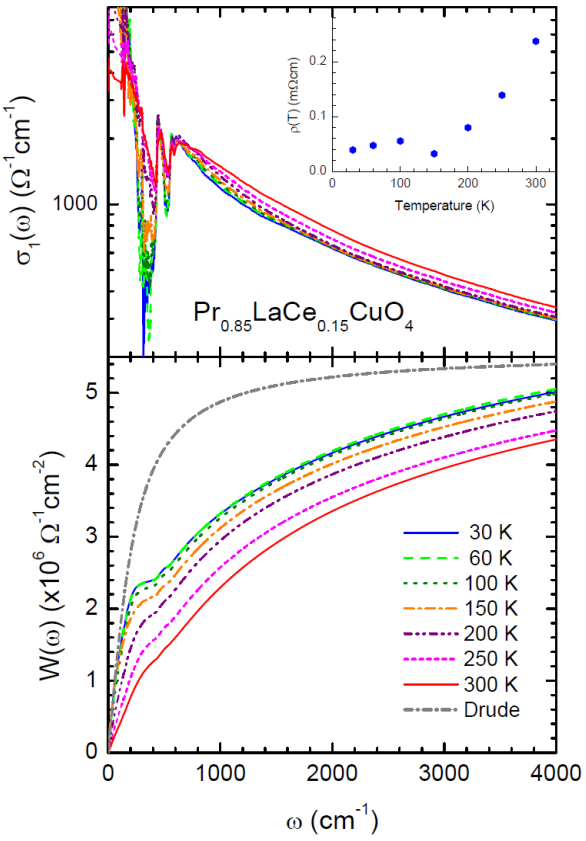

Fig. 2. (Upper frame) The real part of the optical conductivity obtained from the measured reflectance using a Kramers-Kronig analysis. In the inset the extracted DC resistivity from extrapolation to zero frequency is shown. (Lower frame) The partial sums of spectral weight at various temperatures are displayed (see in the text). The gray dash-dotted line is for a simple Drude mode.

temperature the conductivity decreases above 200 cm^{-1} and below the frequency conductivity increases. There is a crossing near 200 cm^{-1}. We extracted the DC resistivity $(\rho(T))$ by extrapolating the optical conductivity to zero frequency. The extracted DC resistivity is displayed in the inset. The DC resistivity decreases monotonically down to 150 K, then increases slightly, and decreases again slowly. This is slightly different from the temperature dependent behavior [16] of $Nd_{1.85}Ce_{0.15}CuO_4$ (NCCO), which is mostly studied electron-doped cuprate system. We also calculated the partial sum (or partial spectral weight) to look up the spectral weight redistribution. The partial sum is defined as follows:

$$\mathrm{W}(\omega) = \int_0^{\omega} \sigma_1(\omega')d\omega'. \quad (1)$$

The obtained partial sums at various temperatures are displayed in the lower frame of Fig. 2. We observe sharp absorption peaks at low frequency range below 200 cm^{-1} which appear steep rises in the partial sum. Overall feature of the partial sum is similar to those of over doped cuprates with holes [20, 21]; as lowering temperature the spectral weight increases in low frequency region below 200 cm^{-1}.

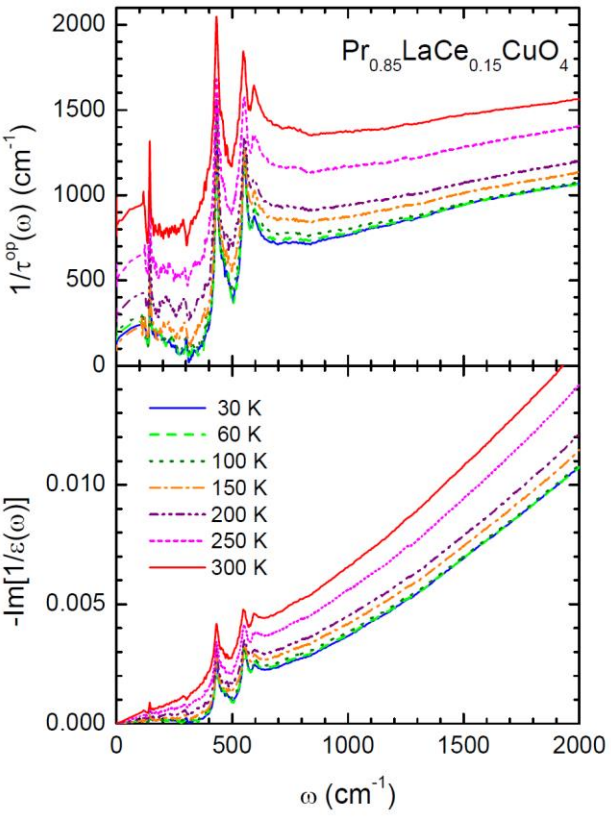

Fig. 3. The optical scattering rate obtained from the optical conductivity through the extended Drude formalism and the energy loss function.

The low-frequency spectral-weight increase can be understood through spectral weight transfer from high frequency to low frequency region. The low temperature partial sum is higher than that at high temperature in a very wide spectral range. This temperature-dependent property of the partial spectral weight seems to be common in both electron- and hole-doped cuprates. We also compare the partial sum with that of a Drude mode (the gray dot-dashed curve) and find that the measured partial sums clearly show strong deviation from the simple Drude behavior (see in the lower frame).

We applied an extended Drude model to investigate the deviation from the Drude model in the optical conductivity. Through this extended Drude model formalism one can extract information on correlation among charge carriers which is very important characteristics to understand strongly correlated electron systems including high-temperature superconductors. The correlation information can be encoded in the optical self-energy ($\tilde{\Sigma}^{op}(\omega)$) which can be defined through the extended Drude model. The optical self-energy can be measured by optical spectroscopy technique and is closely related to the well-known quasiparticle self-energy [22, 23] which can be measured directly using angle-resolved photoemission spectroscopy technique. In the extended Drude model formalism the optical conductivity is related to the optical self-energy as follows [24]:

$$\tilde{\sigma}(\omega) = i\frac{{\omega_p}^2}{4\pi}\frac{1}{\omega - 2\tilde{\Sigma}^{op}(\omega)}. \qquad (2)$$

where $\tilde{\sigma}(\omega)$ is the complex optical conductivity $\left(i.e.\ \tilde{\sigma}(\omega) = \sigma_1(\omega) + i\sigma_2(\omega)\right)$, $\tilde{\Sigma}^{op}(\omega)$ is the complex optical self-energy $\left(i.e.\ \tilde{\Sigma}^{op}(\omega) = \sum_1^{op}(\omega) + i\sum_2^{op}(\omega)\right)$ and ω_p is the plasma frequency of whole (coherent and incoherent) charge carriers in the system. The imaginary part of the optical self-energy is related to the well-known optical scattering rate $\left(i.e. -2\sum_2^{op}(\omega) = 1/\tau^{op}(\omega)\right)$ and the real part is related to the optical effective mass $(m^*(\omega))$ caused by the correlation $(i.e. -2\sum_1^{op}(\omega) = \omega[m^*(\omega)/m_e - 1] = \omega\lambda^{op}(\omega))$, where m_e is the bare electron mass and $\lambda^{op}(\omega)$ the optical mass renormalization constant.

In the upper frame of Fig. 3 we display the optical scattering rate obtained from the optical conductivity through the extended Drude model. The optical scattering rate shows strong sharp peaks which are related to the features of the reflectance spectrum in the similar frequency region. We have performed the usual method used to remove TO phonons to get rid of those peaks from the scattering rate for further analysis. But the method did not work at all and finally we gave it up. This is one of the reasons why we conclude that those peaks are not usual TO phonons. So we assume that those peaks are extrinsic and can be longitudinal optical (LO) phonons. In principle peaks in the energy loss function correspond to the positions of the LO phonons. Therefore, we calculated the energy loss function $(i.e. -Im[1/\tilde{\varepsilon}(\omega)])$, where $\tilde{\varepsilon}(\omega)$ is the complex dynamic dielectric function $\left(i.e.\ \tilde{\varepsilon}(\omega) = \varepsilon_1(\omega) + i\varepsilon_2(\omega)\right)$. We displayed the energy loss function in the lower frame of Fig. 3. We can see that the peaks in the optical scattering rate have the same frequencies and very similar shapes. Therefore we think that the sharp peaks in the scattering rate originate from the LO phonons which are out of plane ($i.e.$ along the c-axis) oscillations.

We tried to remove the peaks in the optical scattering rate for further analysis using the energy loss function.

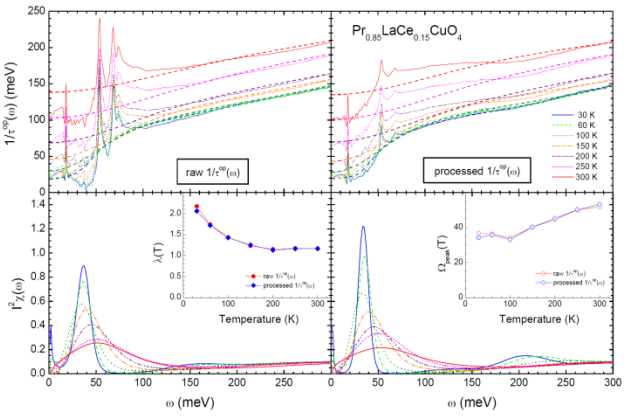

Fig. 4. (Upper frames) The raw and processed (see in the text) optical scattering rates and corresponding fits using the maximum entropy technique in the left and right frames, respectively. (Lower frames) The resulting electron-boson spectral density functions obtained from solving the Shulga *et al.*'s integral equation for the two optical scattering rates.

First we subtracted the slowly increasing background of the energy loss function from the loss function, multiplied an appropriate number (350,000) to the resulting loss, and then subtracted the adjusted loss function from the optical scattering rate. The optical scattering rate obtained through the process is displayed in the upper right frame of Fig. 4. We can see that the sharp peaks are suppressed significantly. We also show the raw optical scattering rates and fits in the upper left frame. In the two frames the dashed lines are fits to the scattering data with the Shulga *et al.*'s formula [10] using a maximum entropy method [12]. The Shulga *et al.*'s formula, which is an extension of the original Allen's formula [8] for analysis of measured data at finite temperatures, can be written as follows:

$$\frac{1}{\tau^{op}(\omega,T)} = \int_0^\infty I^2\chi(\Omega)K(\omega,\Omega;T)d\Omega$$
$$K(\omega,\Omega;T) = \frac{\pi}{\omega}\left[2\omega\coth\left(\frac{\Omega}{2T}\right) - (\omega+\Omega)\coth\left(\frac{\omega+\Omega}{2T}\right) + (\omega-\Omega)\coth\left(\frac{\omega-\Omega}{2T}\right)\right] \quad (3)$$

where $K(\omega,\Omega;T)$ is the kernel for the linear integral equation and T is the temperature in Kelvin unit. We note that the formula can be applicable to data at normal state. By solving the integral equation numerically we obtained the electron-boson spectral density functions $\left(I^2\chi(\omega)\right)$ and showed them for the two (raw and processed) optical scattering rates in the lower two frames of Fig. 4. For the numerical fitting we used a maximum entropy method [11, 12]. This method allows us to obtain the most probable positive electron-boson spectral density function for the measured optical scattering rate. While the processed optical scattering rates at low temperatures up to 100 K are fitted quite well with the generalized Allen's model the scattering rates at high temperatures above 100 K are not fitted well with the model. It seems to be related to LO phonons and the subtraction process. But we do not clearly figure out yet the reason why we have poor fitting quality at high temperatures.

We also obtained temperature dependent coupling constant $\left(\lambda(\omega)\right)$ and peak position $\left(\Omega_{peak}(T)\right)$ from the obtained electron-boson spectral density function. The coupling constant is defined as $\lambda(T) = \int_0^{\omega_c}\frac{I^2\chi(\Omega,T)}{\Omega}d\Omega$, where ω_c is the cutoff frequency which we use 300 meV ($\cong 2400\ \mathrm{cm}^{-1}$). The resulting coupling constants for two (raw and processed) scattering cases agree quite well each other; both show very similar temperature dependencies. The temperature dependencies of coupling constant and peak position are similar to those in hole-doped cuprates [20, 25, 26]. We note that the peak position at our lowest temperature is rather high compared with the superconducting transition temperature (T_c).

4. CONCLUSION

We studied an *n*-doped cuprate, single crystal $Pr_{0.85}LaCe_{0.15}CuO_4$, which is grown by a traveling solvent floating zone technique using an optical furnace. We took *ab*-plane reflectance spectra at various temperatures using an *in-situ* metallization technique and obtained the optical constants using the Kramers-Kronig analysis. The *ab*-plane optical spectra show that they contain the *c*-axis component especially the *c*-axis LO phonons. We observed that our optical conductivity spectra deviate from the simple Drude behavior, which means that our material is a correlated electron system. We applied an extended Drude model to the optical conductivity spectra to get the optical self-energy which can carry the correlation information among charge carriers in the material. Furthermore we used a generalized Allen's formula (or Shulga *et al.* formula [10]) which is a linear integral equation and relates the optical scattering rate (or the imaginary part of the optical self-energy) to the electron-boson spectral density function. By numerically solving the generalized Allen's formula using a maximum entropy method we obtained the electron-boson spectral density function $\left(I^2\chi(\omega)\right)$ from the optical scattering rate. Eventually we calculated temperature-dependent coupling constant (λ) from $I^2\chi(\omega)$ and temperature-dependent broad peak $\left(\Omega_{peak}\right)$ in $I^2\chi(\omega)$ and showed that they are similar to those of hole-doped cuprates. This supports that electron-doped and hole-doped cuprates share a common superconducting mechanism, which may be related to the antiferromagnetic spin fluctuation. But the origin of the spin fluctuation is not figure out yet. The electron-boson spectral density functions of cuprate systems obtained various spectroscopic experimental techniques show universal properties [5], which may help to figure out the origin of the spin fluctuation. This study supplies a piece of evidence that an electron-doped cuprate may fit in the overall picture of the superconducting mechanism of hole-doped cuprates. However, there is a caveat that the peak position at our lowest temperature is rather too high compared with the superconducting transition temperature (T_c). In general the peak energy is proportional to the T_c with a proportionality constant around 6.3 [27]. This issue should be investigated further in the future.

ACKNOWLEDGMENT

The authors acknowledge financial support from the National Research Foundation of Korea (NRFK Grant No. 2013R1A2A2A01067629).

REFERENCES

[1] T. G. Bednorz and A. Muller, "Possible High T_c Superconductivity in the Ba-La-Cu-O System," *Z. Phys. B – Condensed Matter*, vol. 64, pp. 189-193, 1986.

[2] M. R. Norman and C. Repin, "The electronic nature of high temperature cuprate superconductors," *Rep. Prog. Phys.*, vol. 66, pp. 1547-1610, 2003

[3] A. Damascelli, Z. Hussain and Z. –X. Shen, "Angle-resolved photoemission studies of the cuprate superconductors," *Rev. Mod. Phys.*, vol. 75, pp. 473-541, 2003.

[4] D. N. Basov and T. Timusk, "Electrodynamics of high-T_c superconductors," *Rev. Mod. Phys.*, vol.77, pp. 721-779, 2005.
[5] J. P. Carbotte, T. Timusk, and J. Hwang, "Bosons in high temperature superconductors: an experimental survey," *Reports on Progress in Physics*, vol. 74, pp. 066501-1~43, 2011.
[6] H. Takagi, S. Uchida, and Y. Tokura, "Superconductivity produced by electron doping in CuO_2-layered compounds," *Phys. Rev. Lett*., vol. 62, pp. 1197-1200, 1989.
[7] N. P. Armitage, P. Fournier, and R. L. Greene, "Progress and perspectives on electron-doped cuprates," *Rev. Mod. Phys*., vol. 82, pp. 2421-2487, 2010.
[8] J. Hwang, "An analysis method of reflectance spectra of strongly correlated electron systems", *Progress in Superconductivity and Cryogenics*, vol. 15, pp.14~18, 2003.
[9] P. B. Allen, "Electron-phonon effects in the infrared properties of metals," *Phys. Rev. B*, vol. 3, pp. 305-320, 1971.
[10] S. V. Shulga, O. V. Dolgov, and E. G. Maksimov, "Electronic states and optical spectra of HTSC with electron-phonon coupling," *Physica C*, vol. 178, pp. 266-274, 1991.
[11] E. T. Jaynes, "Information theory and statistical mechanics," *Phys. Rev*., vol. 106, pp. 620-630, 1957.
[12] E. Schachinger, D. Neuber, and J. P. Carbotte, "Inversion techniques for optical conductivity data," *Phys. Rev. B*, vol. 73, pp. 184507-1~19, 2006.
[13] D. Song, "Exploring electron-doped cuprate in 4-dimensional phase space by angle resolved photoemission spectroscopy," *Ph. D Thesis*, Yonsei University, 2013.
[14] C. C. Homes, M. Reedyk, D. A. Cradles, and T. Timusk, "Technique for measuring the reflectance of irregular, submillimeter-sized samples," *Appl. Opt*., vol. 32, pp. 2976-2983, 1993.
[15] Y. Onose, Y. Taguchi, K. Ishizaka, and Y. Tokura, "Charge dynamics in underdoped $Nd_{2-x}Ce_xCuO_4$: Pseudogap and related phenomena," *Phys. Rev. B*, vol. 69, pp. 024504-1~13, 2004.
[16] N. L. Wang, G. Li, Dong Wu, X. H. Chen, C. H. Wang, and H. Ding, "Doping evolution of the chemical potential, spin-correlation gap, and charge dynamics of $Nd_{2-x}Ce_xCuO_4$," *Phys. Rev. B*, vol. 73, pp. 184502-1~6, 2006.
[17] E. J. Singley, D. N. Basov, K. Kurahashi, T. Uefuji, and K. Yamada, "Electron dynamics in $Nd_{1.85}Ce_{0.15}CuO_{4+\delta}$: Evidence for the pseudogap state and unconventional *c*-axis response," *Phys. Rev. B*, vol. 64, pp. 224503-1~12, 2001.
[18] T. Startseva, T. Timusk, A. V. Puchkov, D. N. Basov, H. A. Mook, M. Okuya, T. Kimura, and K. Kishio, "Temperature evolution of the pseudogap state in the infrared response of underdoped $La_{2-x}Sr_xCuO_4$," *Phys. Rev. B*, vol. 59, pp. 7184-7190, 1999.
[19] D. B. Tanner and C. D. Poter, "http://www.phys.ufl.edu/tanner/datan.html."
[20] J. Hwang, J. Yang, T. Timusk, S. G. Sharapov, J. P. Carbotte, D. A. Bonn, Ruixing Liang, and W. N. Hardy, "a-axis optical conductivity of detwinnedortho-II $YBa_2Cu_3O_{6.50}$," *Phys. Rev. B*, vol. 73, pp. 014508-1~12, 2006.
[21] J. Hwang, T. Timusk, and G. D. Gu, "Doping dependent optical properties of $Bi_2Sr_2CaCu_2O_{8+\delta}$," *J. Phys.: Condens. Matter*, vol. 19, pp. 125208-1~32, 2007.
[22] J. P. Carbotte, E. Schachinger, and J. Hwang, "Boson structures in the relation between optical conductivity and quasiparticle dynamics," *Phys. Rev. B*, vol. 71, pp. 054506-1~10, 2005.
[23] J. Hwang, E. J. Nicol, T. Timusk, A. Knigavko, and J. P. Carbotte, "High energy scales in the optical self-energy of the cuprate superconductors," *Phys. Rev. Lett*., vol. 98, pp. 207002-1~4, 2007.
[24] J. Hwang, T. Timusk, and G. D. Gu, "High-transition-temperature superconductivity in the absence of the magnetic-resonance mode," *Nature*, vol. 427, pp. 714-717, 2004.
[25] J. Hwang, T. Timusk, E. Schachinger, and J. P. Carbotte, "Evolution of the bosonic spectral density of the high-temperature superconductor $Bi_2Sr_2CaCu_2O_{8+\delta}$," *Phys. Rev. B*, vol. 75, pp. 144508-1~6, 2007.
[26] J. Hwang, "Electron-boson spectral density function of underdoped $Bi_2Sr_2CaCu_2O_{8+\delta}$ and $YBa_2Cu_3O_{6.50}$," *Phys. Rev. B*, vol. 83, pp. 014507-1~7, 2011.
[27] J. Yang,J. Hwang,E. Schachinger, J. P. Carbotte, R. P. S. M. Lobo, D. Colson, A. Forget, and T. Timusk, "Exchange Boson Dynamics in Cuprates: Optical Conductivity of $HgBa_2CuO_{4+\delta}$," *Phys. Rev. Lett*., vol. 102, pp. 027003-1~4, 2009.